Statistical Equilibria of Large Scales in Dissipative Hydrodynamic Turbulence

V. Dallas,[1,2] S. Fauve,[2] and A. Alexakis[2]
[1]Department of Applied Mathematics, University of Leeds, Leeds LS2 9JT, United Kingdom
[2]Laboratoire de Physique Statistique, École Normale Supérieure, CNRS, Université Pierre et Marie Curie, Université Paris Diderot, 24 rue Lhomond, 75005 Paris, France
(Received 8 July 2015; published 11 November 2015)

We present a numerical study of the statistical properties of three-dimensional dissipative turbulent flows at scales larger than the forcing scale. Our results indicate that the large scale flow can be described to a large degree by the truncated Euler equations with the predictions of the zero flux solutions given by absolute equilibrium theory, both for helical and nonhelical flows. Thus, the functional shape of the large scale spectra can be predicted provided that scales sufficiently larger than the forcing length scale but also sufficiently smaller than the box size are examined. Deviations from the predictions of absolute equilibrium are discussed.

DOI: 10.1103/PhysRevLett.115.204501 PACS numbers: 47.27.Ak, 47.27.Gs

Experimental and numerical studies of three-dimensional homogeneous hydrodynamic turbulent flows have been so far mostly focused on the finite energy flux solutions of the Navier-Stokes equations that manifest themselves on scales smaller than the forcing scale for which the Kolmogorov cascade and intermittency take place [1]. This is because the flows of many experiments designed to study statistically stationary turbulent regimes are forced at scales not much smaller than the size of the container. This is also the case of most direct numerical simulations (DNS) for which the flow is often forced in the largest possible modes aiming for the largest scale separation between the forcing scale and the small scales in the dissipative range. A notable exception is of course the limit of two-dimensional flows for which the inverse cascade of energy [2] leads to a negative flux of energy that excites scales larger than the forcing scale.

Many flows of geophysical or astrophysical interest far from the two-dimensional limit involve spatial structures at scales larger than the forcing scale. At these scales, no energy flux is expected and the usual Kolmogorov cascade picture does not hold. This is also true for some flows involved in industrial processes, such as large scale turbulent mixing. Dynamical and statistical properties of the zero flux solutions in scales larger than the forcing scale could thus be of interest for many applications in three-dimensional hydrodynamic turbulence.

Despite the lack of quantitative studies of the large scales in three-dimensional statistically stationary turbulence, it has been believed for a long time that the scales larger than the forcing scale are in statistical equilibrium (see Ref. [1], p. 209). The argument is that the energy driving the flow is transferred from the forcing scale ℓ_f to the dissipation scale ℓ_η by the Kolmogorov cascade and that no mean energy flux exists toward scales larger than ℓ_f. The scales between ℓ_f and the container size L, thus, do not involve any mean energy flux and could be in statistical equilibrium.

With this assumption a k^2 energy spectrum similar to the Rayleigh-Jeans spectrum for blackbody radiation would result with all modes in the range $s2\pi/L < k < 2\pi/\ell_f$ being in equipartition. Such a spectrum was obtained long ago using the Hopf equation for flows without forcing and viscosity [3]. It is also the spectrum obtained in the absence of mean helicity in the truncated Euler equations (i.e., the Euler equations where only Fourier modes with wave numbers $|\boldsymbol{k}| \le k_{\rm cut}$ have been kept, $k_{\rm cut}$ being the truncation wave number) [4]. It should be noted that the steady state problem considered here differs from the one of the large scale structure in decaying turbulence, although a similar spectrum has been predicted [5].

When the initial conditions involve mean helicity H in addition to kinetic energy E, both quadratic invariants need to be taken into account in deriving the energy and helicity distribution among scales for the truncated Euler system. Following the statistical mechanics approach that is usually used to predict absolute equilibria of ideal homogeneous turbulence [6,7], the Boltzmann-Gibbs equilibrium distribution is defined as $\mathcal{P} = Z^{-1}\exp(-\alpha E - \beta H)$, where $Z = \int_\Gamma \exp(-\alpha E - \beta H)d\Gamma$ is the partition function integrated over the phase space Γ and α, β can be seen as the inverse temperatures in the classical thermodynamic equilibrium sense, which are determined by the total energy and the helicity of the system. From there, Kraichnan [2] derived the absolute equilibria of the energy spectrum $E(k)$ and the helicity spectrum $H(k)$, which are

$$E(k) = \frac{4\pi\alpha k^2}{\alpha^2 - \beta^2 k^2} \quad \text{and} \quad H(k) = \frac{8\pi\beta k^4}{\alpha^2 - \beta^2 k^2}, \qquad (1)$$

with $\alpha > 0$ and $\alpha > |\beta| k_{\rm cut}$. These spectra have a singularity at $k = k_s \equiv \alpha/\beta > k_{\rm cut}$ outside the range of validity of Eqs. (1). The ratio $|\beta| k_{\rm cut}/\alpha$ gives a measure of the relative helicity $H(k)/[kE(k)]$ of the flow with 0 corresponding to a

nonhelical flow, and 1 to the fully helical singular case where all energy and helicity is concentrated in the largest wave numbers $|\boldsymbol{k}| = k_{\mathrm{cut}}$. The truncated Euler equations have been widely studied by Brachet and co-workers [8] and the validity of the predicted spectra in Eqs. (1) has been verified. A recent work has also shown that the kinematic dynamo properties of an Arnold-Beltrami-Childress flow forced at small scales compared to the domain size can be well described by modeling the large scales of the flow using the truncated Euler equation [9].

In this Letter we show that despite the fact that in three-dimensional hydrodynamic turbulence the scales between the forcing scale and the container size are not isolated from the turbulent scales, their statistics may still be reasonably approximated as if they were in statistical equilibrium. We consider flows with high enough scale separation by applying helical and nonhelical forcings at intermediate scales using numerical simulations of the forced hyperviscous Navier-Stokes equations and we focus on the dynamical and statistical properties of the large scales.

In laboratory experiments as well as in planets and stars, physical boundaries confine fluids and determine the largest possible length scales. In our DNS, the computational domain is the surrogate for this spatial confinement. For our study it is important to obtain high enough scale separation between the size of our periodic box 2π and the forcing scale while at the same time small scale turbulence is resolved. Forcing at intermediate scales and aiming for a turbulent flow with high enough scale separation is almost prohibitive even with today's supercomputing power. We partly circumvent this difficulty by considering the hyperviscous Navier-Stokes equations under the assumption that the viscous scale should not significantly affect the statistical properties of the large scales. The hyperviscous Navier-Stokes equations then read as

$$\partial_t \boldsymbol{u} + (\boldsymbol{u}\cdot\boldsymbol{\nabla})\boldsymbol{u} = -\boldsymbol{\nabla}P + (-1)^{n+1}\nu_h\boldsymbol{\nabla}^{2n}\boldsymbol{u} + \boldsymbol{f}, \qquad (2)$$

where $\boldsymbol{u}$ denotes the solenoidal velocity field, ν_h is the specified constant hyperviscocity, $\boldsymbol{f}$ is the forcing function, which is described below, and P is the hydrodynamic pressure. Note that for our purposes the hyperviscous term was chosen to take the value of $n = 4$. In the ideal case $\nu_h = 0$ and $\boldsymbol{f} = 0$ Eq. (2) conserves the kinetic energy $E = \frac{1}{2}\langle|\boldsymbol{u}|^2\rangle$ and the helicity $H = \langle\boldsymbol{u}\cdot\boldsymbol{\omega}\rangle$ with $\boldsymbol{\omega} = \boldsymbol{\nabla}\times\boldsymbol{u}$ being the vorticity and the angular brackets denoting a spatial average unless indicated otherwise. The level of helicity in the flow corresponds to the degree of the alignment between the velocity and the vorticity and this is given by the normalized helicity $-1 \le \rho_H \equiv H/(\langle|\boldsymbol{u}|^2\rangle\langle|\boldsymbol{\omega}|^2\rangle)^{1/2} \le 1$.

Using a standard pseudospectral code we numerically solve Eq. (2) satisfying $\boldsymbol{\nabla}\cdot\boldsymbol{u} = 0$. Aliasing errors are removed using the 2/3 rule, i.e., wave numbers $k_{\mathrm{min}} = 1$ and $k_{\mathrm{max}} = N/3$, where N is the number of grid points on each side of the computational box. The temporal integration was performed using a third-order Runge-Kutta scheme. Further details on the code can be found in Ref. [10].

In this study, the velocity field is forced at intermediate wave numbers k_f. The forcing that we consider is a helical random forcing

$$\begin{aligned}\boldsymbol{f}_H = f_0\{&[\cos(k_f y + \phi_y) + \sin(k_f z + \phi_z)]\hat{x},\\ &[\cos(k_f z + \phi_z) + \sin(k_f x + \phi_x)]\hat{y},\\ &[\cos(k_f x + \phi_x) + \sin(k_f y + \phi_y)]\hat{z}\}, \qquad (3)\end{aligned}$$

where $\boldsymbol{f}_H\cdot\boldsymbol{\nabla}\times\boldsymbol{f}_H = |\boldsymbol{k}|\boldsymbol{f}_H^2 > 0$ at each point in space and a nonhelical random forcing

$$\begin{aligned}\boldsymbol{f}_{NH} = f_0\{&[\sin(k_f y + \phi_y) + \sin(k_f z + \phi_z)]\hat{x},\\ &[\sin(k_f z + \phi_z) + \sin(k_f x + \phi_x)]\hat{y},\\ &[\sin(k_f x + \phi_x) + \sin(k_f y + \phi_y)]\hat{z}\}, \qquad (4)\end{aligned}$$

where $\langle\boldsymbol{f}_{NH}\cdot\boldsymbol{\nabla}\times\boldsymbol{f}_{NH}\rangle = 0$. The phases ϕ_x, ϕ_y, ϕ_z were changed randomly at given correlation time scales τ_c. All the necessary parameters of our problem are tabulated below (see Table I). Here we define the Reynolds number based on our control parameters as $\mathrm{Re} \equiv u_f k_f^{1-2n}/\nu_h$, where $u_f \propto (f_0/k_f)^{1/2}$.

Since we are interested in the large scale behavior we need to make sure that our DNS have been integrated long enough so that the largest scales are in a statistically stationary state. In order to illustrate that such states have been reached, we define the energy weighted in the large scales as $M(t) = \sum_{k,k\neq 0} k^{-4}E(k,t)$. M is a large scale quantity and we monitor it as a function of time (see Fig. 1). During the first time steps the very large scales are generated and their energy becomes quickly fairly large [see insets in Figs. 1(a) and 1(b)]. Then, they decay on a much slower time scale. After long enough time integration the large scales reach a stationary state for both helical [Fig. 1(a)] and nonhelical flows [Fig. 1(b)]. In what follows we analyze the data from these saturated states.

Figure 2 presents the energy spectra compensated with k^{-2} [Fig. 2(a)] and the helicity spectra compensated with k^{-4} [Fig. 2(b)]. Note that the energy and helicity spectra

TABLE I. Numerical parameters of the DNS. Note that $\tau_f \equiv (k_{\mathrm{min}} f_0)^{-1/2}$.

k_f	ρ_H	f_0	τ_c/τ_f	ν_h	Re	N
10	0.6	1.0	0.3	5×10^{-12}	6.3×10^{3}	128
20	0.6	2.0	0.15	5×10^{-15}	3.5×10^{4}	256
40	0.6	4.0	0.075	1×10^{-17}	9.7×10^{4}	512
10	0.0	1.0	0.3	5×10^{-12}	6.3×10^{3}	128
20	0.0	2.0	0.15	5×10^{-15}	3.5×10^{4}	256
40	0.0	4.0	0.075	1×10^{-17}	9.7×10^{4}	512

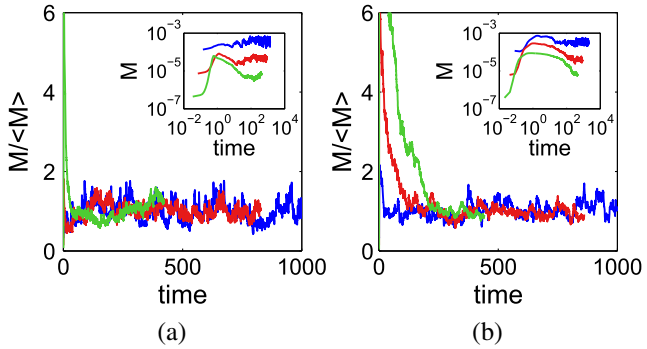

FIG. 1 (color online). Large scale quantity M normalized by its time average $\langle M \rangle$ as a function of time for (a) helical and (b) nonhelical flows. The blue (black) curves denote the runs forced at $k_f = 10$, the red (gray) at $k_f = 20$, and the green (light gray) at $k_f = 40$.

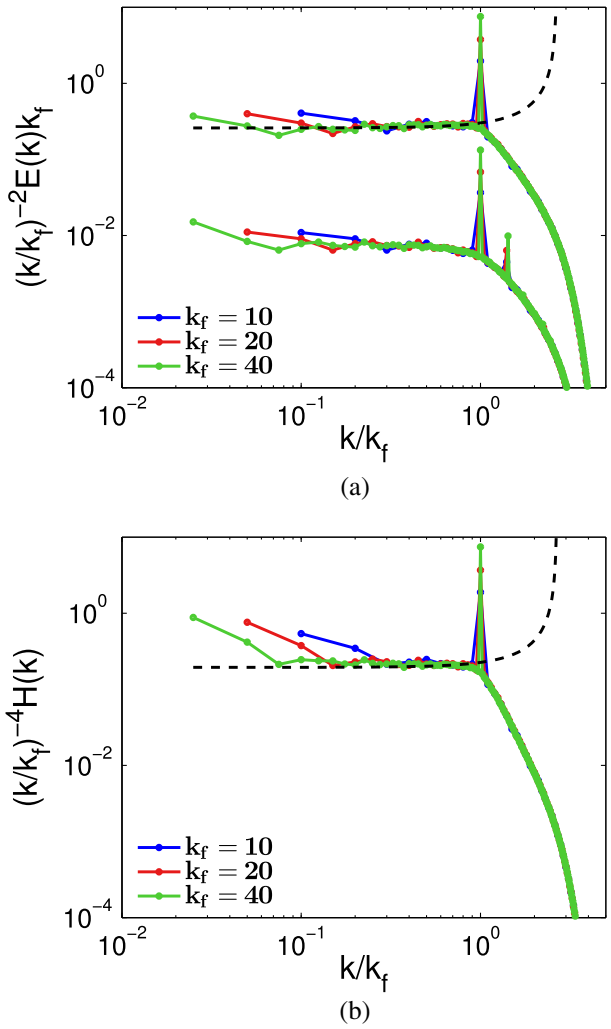

FIG. 2 (color online). (a) Compensated $k^{-2}E(k)$ energy spectra for helical (top) and nonhelical (bottom) flows. (b) Compensated $k^{-4}H(k)$ helicity spectra. The dotted lines represent Kraihnan's absolute equilibria [Eqs. (1)].

collapse since they are rescaled with k/k_f. In Fig. 2(a) the energy spectra for the helical and nonhelical flows are shown with the nonhelical spectra being shifted down for clarity. Our data display a $E(k) \propto k^2$ scaling at low wave numbers $k < k_f$ both for the helical and the nonhelical flows. Similarly, the collapsed helicity spectra in Fig. 2(b) display the scaling $H(k) \propto k^4$. These scalings are in agreement with the absolute equilibria of the truncated Euler equations for helical and nonhelical flows. For comparison to the Kraichnan's theory, we have plotted Eqs. (1) as dotted lines (see Fig. 2) using values of α and β obtained from a linear fit. These curves indicate that the divergence of the spectra predicted by Kraichnan's Eqs. (1) at $k_s = \alpha/\beta$ is expected at $k_s \simeq 2.5k_f$, which is well beyond the expected validity of the absolute equilibrium regime. For this reason no singular behavior is observed deviating from the $H(k) \propto k^4$ scaling and the $E(k) \propto k^2$ power law due to the presence of helicity.

To investigate the effect of helicity in the large scales for the helical runs we plot the relative helicity spectra rescaled with k/k_f in Fig. 3. Kraichnan's absolute statistical equilibria [Eqs. (1)] imply that $(k_f/k)H(k)/[kE(k)]$ is equal to the nondimensional number $2\beta k_f/\alpha = 2k_f/k_s$. This ratio appears to be approximately constant for the highest k_f runs and only for the range of wave numbers $3k_{\min} \leq k < k_f$. The measured value of this ratio in this range gives $2\beta k_f/\alpha \simeq 0.8$, indicating the amount of the relative helicity in the large scales. Despite the fully helical forcing [Eq. (3)] used, not enough helicity has been transferred in the large scales to make the flow fully helical (i.e., $\beta k_f/\alpha = 1$).

Deviations from Eqs. (1) do exist at the largest scales of the system $k \leq 2k_{\min}$. These scales appear to be more energetic and more helical than absolute equilibrium predicts. The amplitude of the deviation is independent of the dissipation mechanism and only weakly dependent

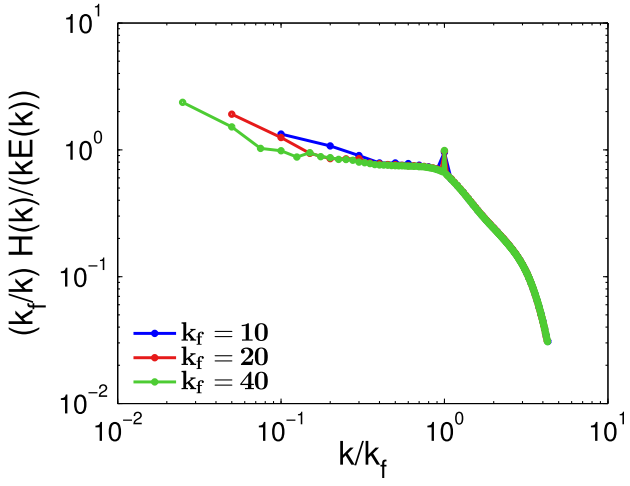

FIG. 3 (color online). Relative helicity spectra $H(k)/[kE(k)]$ rescaled with k/k_f.

on scale separation. There are many possible reasons for this behavior. First, for modes with wavelengths close to the box size the assumptions of isotropy used in the derivation of Eqs. (1) are not valid and deviations from the isotropic result are expected. Another possibility is that a large scale instability could be present [11,12]. Such an instability can transfer energy directly from the forced and turbulent scales to the largest scale of the flow that alters the distribution of energy among modes in the steady state. Such a nonlocal transfer of energy from small to large scales occurs in zonal flows in planetary atmospheres or in plasma physics [13].

At steady state no inverse cascade (negative flux) is expected in three-dimensional hydrodynamic turbulence for either energy or helicity. This is indeed displayed in Fig. 4 which shows the energy flux $\Pi_E(k)$ [Fig. 4(a)] and the helicity flux $\Pi_H(k)$ [Fig. 4(b)] normalized by the energy dissipation rate $\epsilon_E = 2\nu \int_0^\infty k^{2n} E(k,t) dk$ and the helicity dissipation rate $\epsilon_H = 2\nu \int_0^\infty k^{2n} H(k,t) dk$, respectively, for the helical flow with $k_f = 40$. For the wave numbers $k > k_f$ both time-averaged fluxes are positive and constant over the range of $k_f < k < 2.5k_f$, signifying a forward energy and helicity cascade. In the $k < k_f$ range both time-averaged fluxes are zero as expected for absolute equilibria. However, even though the time-averaged $\Pi_E(k)$ and $\Pi_H(k)$ are zero this is not true for the instantaneous fluxes that have large fluctuations of both signs. The power injected by the forcing at $k = k_f$ into the flow fluctuates because both the velocity and the forcing phases are fluctuating. It is thus expected that local couplings generate fluctuations of the energy flux in the shells close to k_f. In addition, Fig. 4 shows that while these fluctuations remain large within the direct cascade, they are strongly damped toward small wave numbers.

In this Letter we investigated to what extent the large scale flow in three-dimensional dissipative hydrodynamic turbulence can be described by the absolute statistical equilibria exhibited from the truncated Euler equations. Using numerical simulations we focus at the spectra of the energy and helicity at large scales. We considered both helical and nonhelical flows which were forced at intermediate wave numbers. For the nonhelical flows we observed a k^2 energy spectrum at large scales, where the energy is equally distributed among the wave numbers $k < k_f$. For the helical flows a k^2 energy spectrum persisted at large scales and the helicity spectrum displayed a k^4 power law at $k < k_f$ in agreement to Kraichnan's theory for ideal helical flows [2].

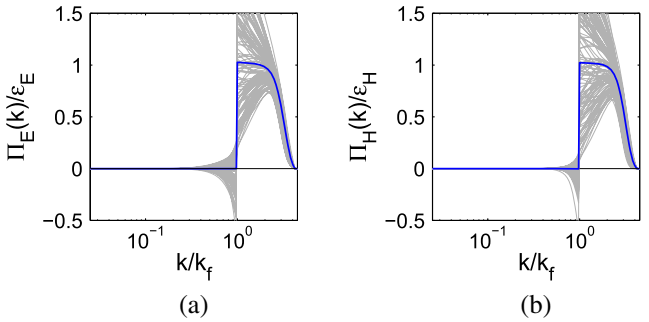

FIG. 4 (color online). (a) $\Pi_E(k)/\epsilon_E$ spectra and (b) $\Pi_H(k)/\epsilon_H$ spectra for the helical flow with $k_f = 40$. Thick blue lines represent the time-averaged values while thin gray lines represent the instantaneous values for various instants in time.

Despite the fully helical forcing used, not enough helicity was transferred in the large scales to allow us to test the singularity of the spectra at $k_s = \alpha/\beta$ which would also distinguish the scaling of the energy spectra between the helical and the nonhelical flows. In absolute equilibria of flows without forcing and dissipation of energy the values of the inverse temperatures are determined by the initial conditions. However, in this dissipative system it is not clear how the system selects these values.

A measurable deviation in the energy and helicity spectra was also observed at the largest scales of the system. Scales of size similar to the box were observed to be more helical and more energetic than the absolute equilibrium predictions. We speculate that these deviations are either due to the absence of isotropy in these scales or due to the presence of a large scale instability.

Energy and helicity fluxes were also investigated. The energy and helicity have a forward cascade for $k > k_f$ and no cascade (zero flux) for $k < k_f$. Notably, even though the time-averaged fluxes are zero, the absolute equilibrium spectra at large scales interact with the forced and dissipative scales through flux fluctuations of the energy and the helicity close to the forcing scale. These interactions are not present in the absolute equilibrium theory that assumes no external sources or sinks of energy and helicity. However, flux fluctuations are also expected in the truncated Euler equations and are responsible for the formation of the Kraichnan spectra. Whether the fluctuations we observe play a subdominant role or they provide a different mechanism for the formation of the k^2 spectra is a question that requires further investigation. Note though that the standard deviation $\sigma(k)$ of these fluctuations decreases like k^4 toward small wave numbers and, hence, they do not feed the excess of energy and helicity observed at the largest scales. Then, one could infer that $\sigma(k)/E(k) \propto (\sqrt{E}/k_f)k^2$ for $k < k_f$ which shows how these fluctuations are related to the Kraichnan spectrum.

To conclude, the present results provide support to the relevance of the absolute equilibrium spectra to the behavior of the large scales in forced dissipative turbulent flows despite the fact that scales between the forcing scale and the domain size ($k < k_f$) are not isolated from the turbulent small scales ($k > k_f$).

The authors acknowledge enlightening discussions with M. E. Brachet. V. D. acknowledges financial support

from the Association DEPHY (Project No. 814443E). The computations were performed using the HPC resources from GENCI-TGCC-CURIE (Project No. x2014056421).

[1] U. Frisch, *Turbulence: The Legacy of A. N. Kolmogorov* (Cambridge University Press, Cambridge, England, 1995).
[2] R. H. Kraichnan, J. Fluid Mech. **59**, 745 (1973).
[3] E. Hopf, J. Rational Mech. Anal. **1**, 87 (1952).
[4] S. A. Orszag, Numerical simulation of turbulent flows, in *Handbook of Turbulence. Volume 1—Fundamentals and Applications*, edited by W. Frost and T. H. Moulden (Springer US, New York, 1977), p. 281.
[5] P. G. Saffman, J. Fluid Mech. **27**, 581 (1967).
[6] H. A. Rose and P. L. Sulem, J. Phys. II (France) **39**, 441 (1978).
[7] J. V. Shebalin, NASA Report No. TP-2002-210783 (2002).
[8] C. Cichowlas, P. Bonaïti, F. Debbasch, and M. Brachet, Phys. Rev. Lett. **95**, 264502 (2005).
[9] S. Gopalakrishnan Ganga Prasath, S. Fauve, and M. Brachet, Europhys. Lett. **106**, 29002 (2014).
[10] D. O. Gómez, P. D. Mininni, and P. Dmitruk, Phys. Scr. T **116**, 123 (2005).
[11] U. Frisch, Z. S. She, and P. L. Sulem, Physica (Amsterdam) **28D**, 382 (1987).
[12] V. Yakhot and G. Sivashinsky, Phys. Rev. A **35**, 815 (1987).
[13] P. H. Diamond, S.-I. Itoh, K. Itoh, and T. S. Hahm, Plasma Phys. Controlled Fusion **47**, R35 (2005).